Journal of Alloys and Compounds 580 (2013) S40–S43

Contents lists available at SciVerse ScienceDirect

Journal of Alloys and Compounds

journal homepage: www.elsevier.com/locate/jalcom

Hydrogen absorption in thin ZnO films prepared by pulsed laser deposition

O. Melikhova [a,*], J. Čížek [a], F. Lukáč [a], M. Vlček [a], M. Novotný [b], J. Bulíř [b], J. Lančok [b], W. Anwand [c], G. Brauer [c], J. Connolly [d], E. McCarthy [d], S. Krishnamurthy [d], J.-P. Mosnier [d]

[a] Charles University in Prague, Faculty of Mathematics and Physics, V Holesovickach 2, CZ-180 00 Praha 8, Czech Republic
[b] Institute of Physics, Academy of Sciences of the Czech Republic, Na Slovance 2, 182 21 Prague, Czech Republic
[c] Institut für Strahlenphysik, Helmholtz-Zentrum Dresden-Rossendorf, PO Box 510 119, D-01314 Dresden, Germany
[d] National Centre for Plasma Science and Technology, School of Physical Sciences, Glasnevin, Dublin 9, Ireland

ARTICLE INFO

Article history:
Available online 7 February 2013

Keywords:
ZnO
Thin films
Hydrogen
Positron annihilation
Defects

ABSTRACT

ZnO films with thickness of ~80 nm were grown by pulsed laser deposition (PLD) on MgO (1 0 0) single crystal and amorphous fused silica (FS) substrates. Structural studies of ZnO films and a high quality reference ZnO single crystal were performed by slow positron implantation spectroscopy (SPIS). It was found that ZnO films exhibit significantly higher density of defects than the reference ZnO crystal. Moreover, the ZnO film deposited on MgO substrate exhibits higher concentration of defects than the film deposited on amorphous FS substrate most probably due to a dense network of misfit dislocations. The ZnO films and the reference ZnO crystal were subsequently loaded with hydrogen by electrochemical cathodic charging. SPIS characterizations revealed that absorbed hydrogen introduces new defects into ZnO.

1. Introduction

Zinc oxide (ZnO) is a wide band gap (3.37 eV) material with numerous applications, including optoelectronic devices, transparent conducting oxides and gas sensors [1]. Ultraviolet lasing emission observed in epitaxial ZnO films stimulated a great interest in preparation of high-quality ZnO films [2]. Majority of ZnO films and crystals exhibit n-type conductivity. On the other hand, acceptor doping leading to p-type conductivity in ZnO remains still unresolved. Theoretical work by Van de Walle [3] showed that hydrogen is easily incorporated into ZnO lattice and should act as a shallow donor. Indeed hydrogen was found to be the most important impurity in high quality ZnO crystals grown by the state-of-art techniques [4]. Weber et al. [5] clearly demonstrated that presence of hydrogen in oxygen deficient ZnO leads to red coloration of initially transparent crystal. This effect has attributed hydrogen interaction with oxygen vacancies [6]. Hence, knowledge about hydrogen behaviour in ZnO lattice and its interaction with intrinsic defects is important for understanding of electrical and optical properties of ZnO. In this work positron annihilation was employed for characterization of structural changes caused by hydrogen absorbed in ZnO.

2. Experimental

ZnO films were deposited by PLD using a frequency-quadrupled Nd:YAG laser operating at the repetition rate of 10 Hz and providing energy of 90 mJ in 6 ns light pulses with wavelength of 266 nm. Laser pulses ablated ultra-high purity ZnO ceramic target with a fluence on target of 2.8 J cm^{-2}. ZnO films were grown as a result of 5200 laser shots on MgO (1 0 0) and FS substrates kept at a temperature of 300 °C in oxygen atmosphere with a pressure of 10 Pa. Film thickness calculated from measurement of optical reflectance and transmittance is (81 ± 3) nm and (75 ± 3) nm for ZnO film deposited on MgO and FS, respectively. A hydrothermally grown bulk ZnO (0 0 0 1) single crystal with O-terminated surface supplied by MaTecK GmbH was used as a reference bulk material.

ZnO films and also the reference single crystal were characterized in the virgin state and then were covered by a 20 nm thick Pd over-layer, which makes the surface conductive and facilitates hydrogen uptake into ZnO [7]. The samples were subsequently doped with hydrogen by cathodic charging in an electrochemical cell filled by a mixture of H_3PO_4 and glycerine in the ratio 1:2. It has been demonstrated previously [8] that this procedure enables to introduce a high amount of hydrogen (at least 30 at.%) into ZnO. Hydrogen charging was performed by constant current pulses applied between a Pt counter electrode and the loaded sample. The current density on surface of the loaded sample was 0.3 mA cm^{-2} and the loading time was adjusted so that the hydrogen concentration introduced into the sample estimated from the transported charge using the Faraday's law was ≈30 at.%.

SPIS investigations were performed on a slow positron beam SPONSOR [9] with energy of incident positrons adjustable in the range from 0.03 to 36 keV. Doppler broadening (DB) of annihilation photopeak was measured by a HPGe detector with an energy resolution of (1.09 ± 0.01) keV at 511 keV. Evaluation of DB was performed using the line shape S parameter. The central energy region for calculation of S was chosen as $|E - m_0c^2| < 0.93$ keV. All S parameters presented in this paper are normalized to the bulk value $S_0 = 0.5068(5)$ determined in the virgin reference ZnO crystal at positron energy of 35 keV.

* Corresponding author. Tel.: +420 221912788.
E-mail address: oksivmel@yahoo.com (O. Melikhova).

0925-8388/$ - see front matter © 2013 Elsevier B.V. All rights reserved.
http://dx.doi.org/10.1016/j.jallcom.2013.01.121

3. Results and discussion

X-ray diffraction (XRD) characterization reported in details in Ref. [10] revealed that both ZnO films exhibit wurtzite ZnO structure and *c*-orientation, i.e. (0001) plane parallel with the substrate. The lattice parameters determined by XRD are comparable with those given for ZnO in literature. The ZnO films deposited on single-crystalline MgO substrate exhibit local epitaxy, while the ZnO film deposited on amorphous FS substrate exhibits (0001) fibre texture with a random lateral orientation of crystallites in the plane of substrate. The size of crystallites determined by scanning electron microscopy falls into the range 30–100 nm and 20–50 nm for ZnO films deposited on MgO and FS substrate, respectively.

Fig. 1a shows dependence of the *S* parameter on positron energy *E* for the reference ZnO (0001) single-crystal. At the lowest energy virtually all positrons annihilate on the ZnO crystal surface. With increasing energy positrons penetrate progressively deeper into the ZnO crystal and the fraction of positrons diffusing back to the surface decreases, ultimately yielding a bulk value corresponding to the situation when all positrons annihilate in the ZnO bulk. The $S(E)$ curve for the virgin crystal can be expressed as $S(E) = S_{surf}[1 - F(E)] + S_0F(E)$, where S_{surf} and S_0 stand for the *S*-parameter for positrons annihilated on the surface and inside ZnO bulk, respectively. The fraction of positrons annihilated in ZnO bulk, $F(E)$, was calculated as a solution of positron diffusion–annihilation equation in a single layer system shown in Fig. 1b by grey area. The model curve obtained from fitting of experimental points by VEPFIT software package [11] is plotted in Fig. 1a by solid line and obviously describes the experimental points accurately. The mean positron diffusion length of (58 ± 2) nm obtained from fitting is in a reasonable agreement with the positron diffusion length determined in a ZnO single crystal in Ref. [12], but is significantly shorter than the mean positron diffusion length of about 100–200 nm typical for nearly defect-free semiconductors [13]. This can be explained by positron trapping in complexes consisting of Zn-vacancy associated with hydrogen atom (V_{Zn} + H) detected in ZnO single crystal by positron lifetime spectroscopy [4]. Indeed, nuclear reaction analysis revealed that hydrogen introduced into ZnO crystal unintentionally during the crystal growth is present in concentration of ≈0.03 at.% and represents, thereby, the most important impurity in the virgin ZnO crystals [14].

Full points in Fig. 1b shows the $S(E)$ curve for ZnO crystal electrochemically charged with hydrogen. From inspection of Fig. 1b it becomes clear that hydrogen loading causes a remarkable increase of the *S* parameter in the whole energy range indicating that new defects were introduced by absorbed hydrogen. Moreover, the shape of the $S(E)$ curve was changed and a shoulder with very high *S* values appeared in the energy range 1–10 keV. This testifies that a sub-surface region with very high density of defects was formed. Theoretical modelling showed that hydrogen absorbed in ZnO causes remarkable lattice expansion [3]. At very low hydrogen concentration this is accumulated by elastic deformation. However, when hydrogen-induced stresses exceed the yield stress in ZnO plastic deformation takes place and introduces new defects into the sample. Since ZnO is relatively soft material [1] the onset of plastic deformation occurs already at low hydrogen concentrations (a few at.%). During electrochemical hydrogen loading there is a large excess of hydrogen concentration on the loaded size covered with Pd. Hydrogen penetrates into ZnO through Pd over-layer and diffuses deeper and deeper into ZnO due to the concentration gradient. As a consequence hydrogen-induced plastic deformation takes place mainly in a sub-surface region below the Pd cap which is characterized by increased *S* parameter. Hydrogen-induced plastic deformation in the sub-surface region causes typical surface modification in the form of hexagonally shaped pyramids formed by hydrogen-induced slip in the *c*-direction [6]. The $S(E)$ curve for hydrogen-loaded ZnO crystal can be described by expression $S(E) = S_{surf}[1 - F_{Pd}(E) - F_{ZnO\text{-}sub\text{-}surf}(E) - F_{ZnO}(E)] + S_{Pd}F_{Pd}(E) + S_{ZnO\text{-}sub\text{-}surf}F_{ZnO\text{-}sub\text{-}surf}(E) + S_{ZnO}F_{ZnO}(E)$, where S_{Pd}, $S_{ZnO\text{-}sub\text{-}surf}$ and S_{ZnO} are *S*-parameters for Pd cap, defected sub-surface region and ZnO bulk, respectively, while F_{Pd}, $F_{ZnO\text{-}sub\text{-}surf}$ and F_{ZnO} denote the fraction of positrons annihilated in the Pd cap, sub-surface region and ZnO bulk, respectively. The $S(E)$ curve for hydrogen loaded crystal was again fitted by a model function calculated now for a three-layer structure shown in Fig. 1b by grey area and consisting of (i) Pd over-layer, (ii) defected sub-surface region and (iii) ZnO bulk. The model curve obtained from fitting is plotted in Fig. 1b by a solid line and agrees well with experimental points. Thickness of the defected sub-surface region obtained from fitting

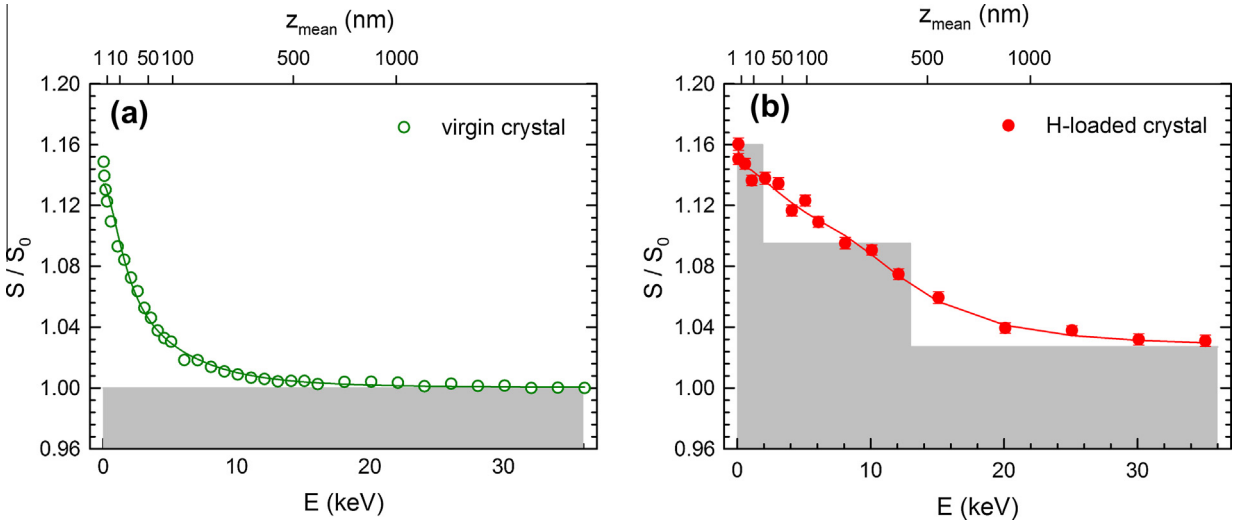

Fig. 1. The dependence of the *S* parameter on energy *E* of incident positrons for the ZnO (0001) single crystal: (a) virgin crystal (prior to deposition of Pd cap); (b) hydrogen loaded crystal. The mean positron penetration depth z_{mean} is shown on the upper horizontal axis. Solid lines show model curves calculated by VEPFIT software for a structure shown in the figure by grey area and consisting of a single layer model for the virgin crystal (a) and a three-layer model for hydrogen loaded crystal (b).

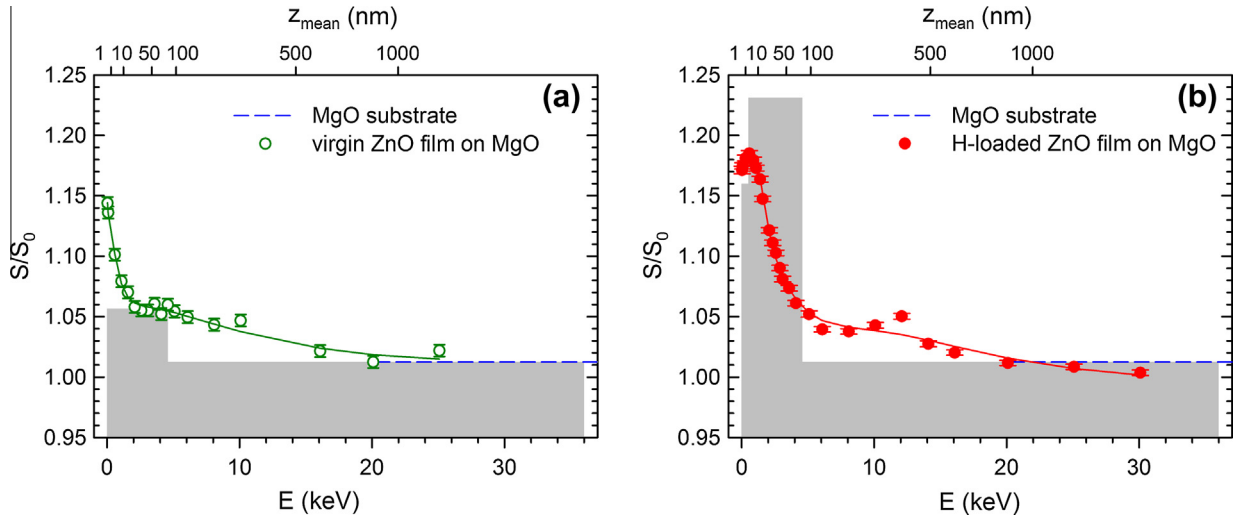

Fig. 2. The $S(E)$ curves for ZnO film deposited on MgO (1 0 0) substrate: (a) virgin film (prior to deposition of Pd cap); (b) hydrogen loaded film. The mean positron penetration depth z_{mean} is shown on the upper horizontal axis. Solid lines show model curves calculated by VEPFIT software for a layered structure shown by grey areas. Dashed lines indicate the bulk S parameter for MgO measured on a bare substrate.

is (430 ± 30) nm. Positron diffusion length in hydrogen loaded crystal was shortened to (20 ± 5) and (42 ± 5) nm for the subsurface region and the bulk, respectively. Shortening of positron diffusion length together with increase of S give a clear evidence for increase of defect concentration due to hydrogen-induced plastic deformation.

Dependence of the S parameter on positron energy E for the virgin ZnO films deposited on MgO and FS substrate is plotted in Figs. 2a and 3a, respectively. At the lowest energy positrons again annihilate on the film surface. With increasing energy positrons become to annihilate in the ZnO layer. Finally at $E > 5$ keV positrons start to penetrate into MgO or FS substrate and the S parameter converges to the bulk value characteristic for each substrate. Hence, the $S(E)$ curve can be described by expression $S(E) = S_{surf}[1 - F_{ZnO}(E) - F_{substrate}(E)] + S_{ZnO} F_{ZnO}(E) + S_{substrate} F_{substrate}(E)$, where S_{ZnO} and $S_{substrate}$ denote the S-parameter for positrons annihilated in ZnO film and in the corresponding substrate, respectively, while F_{ZnO} and $F_{substrate}$ represents the fraction of positrons annihilated in ZnO film and the substrate. The bulk S-parameters $S_{substrate}$ measured on bare MgO and FS substrates, respectively, are indicated in Figs. 2 and 3 by dashed lines. The $S(E)$ curves for the virgin ZnO films were fitted by a model function consisting of (i) ZnO layer and (ii) substrate and the model functions are plotted in Figs. 2a and 3a by solid lines. The thicknesses of ZnO layer obtained from fitting are (80 ± 2) nm and (76 ± 1) nm for the film deposited on MgO and FS substrate, respectively, and agree well with those calculated from measurement of optical reflectance and transmittance and also with thicknesses determined by X-ray reflectivity measurements [8]. The S parameters for the ZnO layer S_{ZnO} obtained from fitting are compared in Fig. 4. Obviously both virgin ZnO films exhibit higher S-parameter than the virgin ZnO crystal indicating higher concentration of defects. The virgin ZnO films likely contain point defects similar to those in the reference ZnO single crystal, i.e. V_{Zn} + H complexes. In addition, they contain also misfit dislocations compensating the lattice mismatch between the film and the substrate, and open-volume defects at grain boundaries or interfaces between various crystallites. In the ZnO film deposited on FS substrate the mismatch between atomic positions

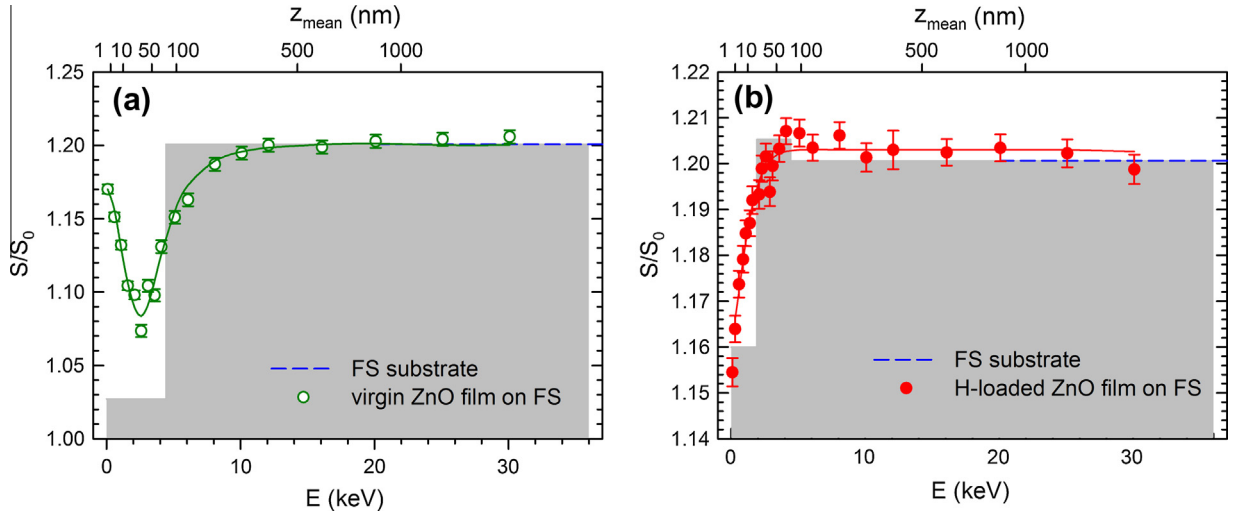

Fig. 3. The $S(E)$ curves for ZnO film deposited on FS substrate: (a) virgin film (prior to deposition od Pd cap); (b) hydrogen loaded film. The mean positron penetration depth z_{mean} is shown on the upper horizontal axis. Solid lines show model curves calculated by VEPFIT software for a layered structure shown by grey areas. Dashed lines indicate the bulk S parameter for FS measured on a bare substrate.

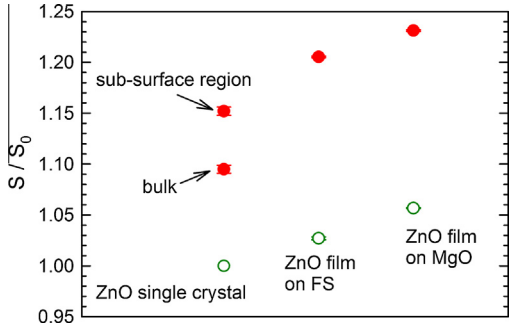

Fig. 4. The S parameters for ZnO crystal and thin films obtained from fitting of $S(E)$ curves: open points – virgin samples; full points – hydrogen loaded samples. In case of ZnO (0001) single crystal the S parameter for the defected sub-surface region and for the bulk ZnO region are shown.

in the substrate and in the film is to some extend compensated for by many differing orientations (tilting) of the ZnO crystallites. As a consequence, the density of misfit dislocations in the ZnO film deposited on FS substrate is lower than in the film deposited on MgO substrate which exhibits local epitaxy and the lattice mismatch with substrate is accumulated mainly by misfit dislocations.

The $S(E)$ curves for hydrogen loaded ZnO films deposited on MgO and FS substrate are plotted in Figs. 2b and 3b, respectively. The $S(E)$ curve for hydrogen loaded film is described by the expression $S(E) = S_{surf}\,[1 - F_{Pd}(E) - F_{ZnO}(E) - F_{substrate}(E)] + S_{Pd}\,F_{Pd}(E) + S_{ZnO}\,F_{ZnO}(E) + S_{substrate}\,F_{substrate}(E)$, where S_{Pd}, S_{ZnO} and $S_{substrate}$ are S-parameters for Pd over-layer, ZnO film and substrate, respectively, and the symbols $F_{Pd}(E)$, $F_{ZnO}(E)$ and $F_{substrate}(E)$ denote the fractions of positrons annihilated in Pd over-layer, ZnO film and corresponding substrate. Similarly to the bulk ZnO crystal absorption of hydrogen in ZnO films leads to a large increase of S_{ZnO} and simultaneously shortening of the positron diffusion length. One can see in Fig. 4 that hydrogen loaded ZnO films exhibit S_{ZnO} values which are even higher than the S-parameter for the defected sub-surface region in the ZnO crystal. This testifies that hydrogen absorbed in ZnO films causes plastic deformation which introduces a lot of new defects into the films. Contrary to the reference ZnO crystal which exhibits defected sub-surface layer and the remaining bulk region with lower density of defects, in thin ZnO films loaded with hydrogen the defected layer covers the whole film.

4. Conclusions

Very thin ZnO films deposited by PLD and a high quality ZnO single crystal were electrochemically loaded with hydrogen. Structural changes caused by absorbed hydrogen were characterized by SPIS. Hydrogen absorbed in ZnO causes plastic deformation both in the ZnO films and in the ZnO single crystal. Hydrogen-induced plastic deformation is visualized by a typical surface modification and creates a sub-surface region with very high density of defects in the ZnO crystal. In hydrogen loaded ZnO films hydrogen-induced plastic deformation occurs as well and very high density of defects is formed in the whole film.

Acknowledgements

This work was supported by the Czech Science agency (project P108/11/0958), the Ministry of Education, Youths and Sports of the Czech Republic (projects MEB101102 and LH12173), the Charles University in Prague (project SVV-2012-265303) and the German Academic Exchange Service (project 71 31 308 022).

References

[1] D.C. Look, Mater. Sci. Eng. B 80 (2001) 383.
[2] Ü. Özgür, Ya.I. Alivov, C. Liu, A. Teke, M.A. Reshchikov, S. Doğan, V. Avrutin, S.-J. Cho, H. Morkoç, J. Appl. Phys. 98 (2005) 041301.
[3] C.G. Van de Walle, Phys. Rev. Lett. 85 (2000) 1012.
[4] G. Brauer, W. Anwand, D. Grambole, J. Grenzer, W. Skorupa, J. Čížek, J. Kuriplach, I. Procházka, C.C. Ling, C.K. So, D. Schulz, D. Klimm, Phys. Rev. B 79 (2009) 115212.
[5] M.H. Weber, N.S. Parmar, K.A. Jones, K.G. Lynn, J. Electron. Mater. 39 (2010) 573.
[6] M.H. Weber, K.G. Lynn, J. Phys. Conf. Ser. 262 (2011) 012063.
[7] R. Kirchheim, F. Sommer, G. Schluckebier, Acta Metall. 30 (1982). 1982.
[8] J. Čížek, N. Žaludová, M. Vlach, S. Daniš, J. Kuriplach, I. Procházka, G. Brauer, W. Anwand, D. Grambole, W. Skorupa, R. Gemma, R. Kirchheim, A. Pundt, J. Appl. Phys. 103 (2008) 053508.
[9] W. Anwand, H.R. Kissener, G. Brauer, Acta Phys. Pol. A 88 (1995) 7.
[10] M. Novotný, J. Čížek, R. Kužel, J. Bulíř, J. Lančok, J. Connolly, E. McCarthy, S. Krishnamurthy, J.-P. Mosnier, W. Anwand, G. Brauer, J. Phys. D: Appl. Phys. 45 (2012) 225101.
[11] A. van Veen, H. Schut, M. Clement, J. de Nijs, A. Kruseman, M. Ijpma, Appl. Surf. Sci. 85 (1995) 216.
[12] T. Koida, A. Uedono, A. Tsukazaki, T. Sota, M. Kawasaki, S.F. Chichibu, Phys. Status Solidi (a) 201 (2004) 2841.
[13] R. Krause-Rehberg, H.S. Leipner, Positron Annihilation Semiconductor – Defect Studies, Springer, Berlin, 1999.
[14] J. Čížek, F. Lukáč, M. Vlček, I. Procházka, F. Traeger, D. Rogalla, H.-W. Becker, Defect Diffus. Forum 326–328 (2012) 459.